CARBON NANOTUBE REINFORCED Al6061 AND Al2124 NANOCOMPOSITES

N. Saheb[1, 2*], A. Khalil[1], A. S. Hakeem[2], T. Laoui[1, 2], N. Al-Aqeeli[1, 2]

[1]*Department of Mechanical Engineering*
[2]*Center of Excellence in Nanotechnology*
King Fahd University of Petroleum and Minerals, Dhahran – 31261, Saudi Arabia
[*]*nouari@kfupm.edu.sa*

Keywords: Aluminum alloys, carbon nanotubes, nanocomposites, spark plasma sintering

Abstract
In the present work, wet ball milling and spark plasma sintering were used to develop carbon nanotube (CNT) reinforced Al6061 and Al2124 nanocomposites which have potential applications in aerospace and automotive industries. Al6061 and Al2124 nanocomposite powders containing 1 and 2 wt. % CNTs prepared through sonication and wet ball milling were spark plasma sintered at 400, 450, and 500 ℃ for 20 minutes under a pressure of 35 MPa. In case of 1 wt. % content, CNTs were found to have better dispersion and less agglomeration. The increase of CNT content to 2 wt. % resulted in formation of CNT clusters and hence their inhomogeneous distribution across the matrix. Composites reinforced with 1 wt. % CNTs displayed better densification compared to composites containing 2 wt. % CNTs. However, almost full densification was achieved for both composites at 500 ℃. Maximum hardness was found for composites containing 1 wt. % CNTs. For composites containing 2 wt. % CNTs, hardness was found to be lower than that of the monolithic alloys.

1 Introduction

Carbon Nanotubes (CNTs), discovered by Iijima [1], and proved exceptionally strong by Wong and co-workers [2], have been manifested as very promising nanoreinforcements for enhancing various mechanical and physical properties of different metallic and non-metallic materials. Among metallic materials, aluminum and its alloys have gained significant attention for this purpose due to their low densities and wide range of engineering applications. However, uniform distribution of CNTs during mixing and consolidating the composite powder to full densification remained major challenges in the development of CNT reinforced metal matrix nanocomposites. Although few researchers [3-4] reported unsatisfactory improvement in the mechanical properties of aluminum as a result of CNTs addition; other reported dramatic improvement in the properties [5-8]. The mechanical properties of Al\CNT composites were found to be sensitive to CNTs content, as well as, the consolidation technique(s) [9-12].

Mechanical alloying has been used for uniform dispersion of the reinforcement in the matrix and to overcome the problem of agglomeration. Mechanical alloying, also called ball milling, is a powder metallurgy technique which involves mixing, cold welding, breaking and re-welding of powder particles during milling. It is also used to synthesize a variety of materials including

nanocomposites. It has many benefits as a processing technique which includes being simple, versatile and economically feasible.

It is equally vital to consolidate the composite powder using a technique which yield fully dense product and prevent grain growth during sintering. In this regard, spark plasma sintering (SPS) is a unique consolidation technique to produce fully dense metallic materials at relatively low sintering temperature, short sintering time, and fast heating rate [13-14]. This results the retention of fine microstructures and high densification of SPS'ed compacts. In addition, SPS is not only a binder-less process but also does not require a pre-compaction step.

In previous work, we investigated the effect of sintering temperature, time and pressure on the densification and hardness of spark plasma sintered Al6061 and Al2124 aluminum alloys [15-16]. Also, we prepared CNT reinforced Al6061 and Al2124 nanocomposite powders through sonication and wet milling [17]. The objective of the present work is to develop CNT reinforced Al6061 and Al2124 nanocomposites through wet ball milling and SPS. The microstructure, density and hardness of the nanocomposites will be characterized as function of CNT content and sintering temperature.

2 Materials and Methods

The Al6061 and Al2124 pre-alloyed powders were used in this study and were supplied by the Aluminum Powder Co. Ltd. The chemical composition of both aluminum alloys is shown in table 1. CNTs having diameter of around 50 nm and length of few microns were used as reinforcement. Al2124 and Al6061 powders containing 0, 1 and 2 wt. % CNTs were prepared through wet ball milling using a Fritsch P5 planetary ball mill. CNTs were sonicated via probe sonicator for 30 minutes in ethanol and then the pre-alloyed powder was added followed by further sonication of the mixture for 15 minutes. The sonicated slurry was charged into cylindrical stainless steel vials (250 ml in volume) together with stainless steel balls and wet milled for 1 hour. The wet milling was carried out at room temperature at a speed of 200 rpm in argon inert atmosphere to prevent the oxidation of the powders. A ball to powder weight ratio of 10:1 was used.

Powder	Fe	Si	Cu	Mn	Mg	Zn	Al
Al6061	0.192	0.69	0.29	0.016	0.83	0.012	Bal.
Al2124	0.064	0.058	3.88	0.58	1.42	0.034	Bal.

Table 1. Chemical composition of starting powders in weight percent.

Fully automated spark plasma sintering equipment (FCT system, model HP D 5, Germany) was used to sinter the samples. The dried nanocomposite powders were directly charged into graphite die through which the current is passed. A 20 mm diameter graphite die was used and a pressure of 35 MPa was applied during the whole sintering process, i.e., during heating and holding time. The heating rate was 100 °C/min. The samples were sintered under vacuum at 400, 450, and 500 °C for 20 minutes. Scanning electron microscope (SEM) was used to characterize the raw powders and analyze the microstructure of sintered samples. The density of sintered samples was measured using Alfa Mirage electronic densimeter (model MD-300s). Vickers microhardness of the spark plasma sintered samples was measured using MMT-3 digital microhardness tester. All measurements were taken at a load of 100 gf and the indenter dwell time was 12 seconds.

3 Results and Discussion

Figure 1 shows the morphology of as received powders. It can be seen that the powders are composed of particles having various shapes and sizes. Morphology of CNTs used in this study is shown in figure 2 where it can be seen that CNTs are in fairly separated state without excessive clustering. Morphology of composite aluminum powders after ball milling is shown in figure 3.

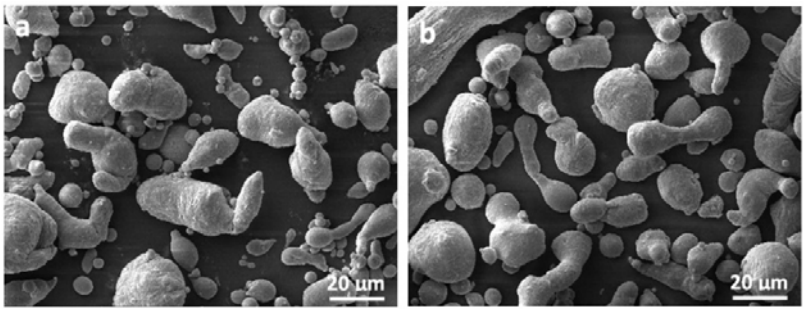

Figure 1. Morphology of as received powders of (a) Al2124 and (b) Al6061

It is evident that CNTs are less agglomerated; uniformly dispersed, and have good adhesion to the matrix for composites containing 1 wt. % CNTs, however, inhomogeneous distribution and clustering of CNTs is more pronounced for composites containing 2 wt. % CNTs. Almost similar trend was observed for Al2124 composite powders. The clustering of CNTs is being constantly observed and reported [4-12] and found highly undesirable because these agglomerates hinder proper neck growth between adjacent matrix particles during sintering and hence cause poor densification and mechanical properties of the composite material [6].

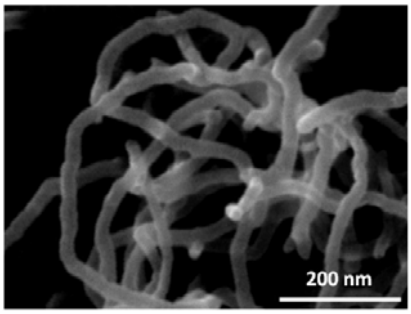

Figure 2. Morphology of as received CNTs.

Uniform dispersion of CNTs requires careful design of dispersion techniques and routes to have maximum benefit from these extremely strong reinforcements. The combination of sonication and wet milling used in this work improved CNTs dispersion which led to their uniform distribution in composite containing 1 wt. % of CNTs. However, considerable agglomeration was observed in the composite containing 2 wt. % CNTs which caused poor hardness of the composites as discussed below.

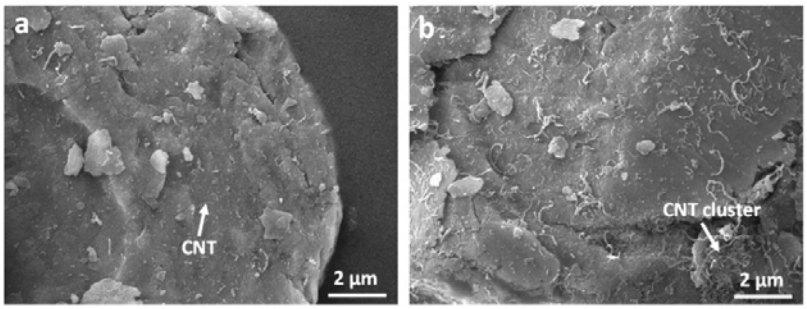

Figure 3. Morphology of Al6061 powders containing (a) 1 wt. % and (b) 2 wt. % CNTs

Particles size distribution of as-received and powders milled for 1 hour, is shown in figure 4. It can be seen that frequency of the distribution changed after milling and curves of the graph slightly shifted towards smaller particle size. It was observed that average particle of as received Al6061 and Al2124 aluminum powders are 50 and 35 µm, respectively.

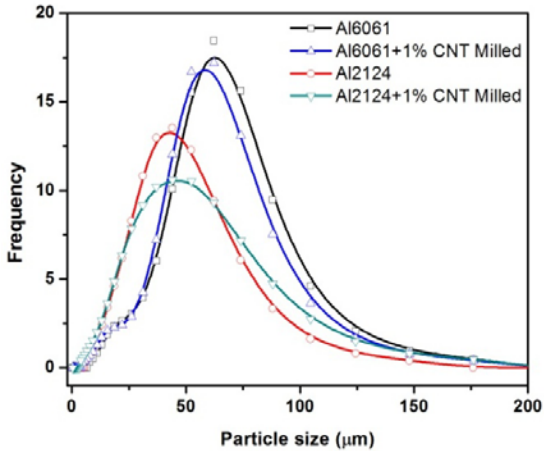

Figure 4. Particle size distribution of as received and ball milled composite powders.

Figure 5 (a) shows x-ray diffractograms (XRD) of as received Al6061 and Al2124 powders and composite powders before sintering. Figure 5 (b) shows XRD peaks of sintered Al6061 and its nanocomposites. There is no evidence of the presence of phases such as Al_4C_3 or other carbides which may form during sintering.

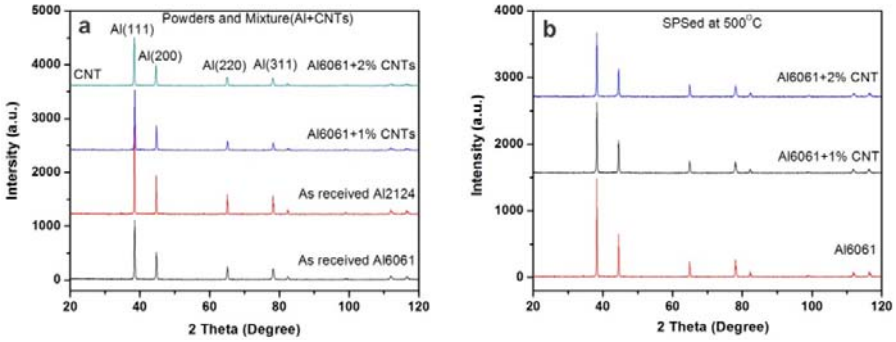

Figure 5. (a) X-Ray Diffractograms for the Al6061 and Al2124 powders and there composites. (b) SPS'ed Al6061 and its nanocomposites containing 1 and 2 wt % CNTs, specimens were sintered at 500 °C.

Figure 6 shows SEM micrographs of SPS'ed Al6061 specimens sintered at 450 °C with varying CNT content. No pores were found in the monolithic matrix, as shown in figure 6 (a). Whereas, increasing porosity can be seen in nanocomposites with increasing CNT content from 1 to 2 wt. % as shown in the figure 6 (b and c), respectively. Figure 6 (d) shows the magnified SEM micrograph of one of the pores which are visible in figure 6 (c). The pores are composed of CNTs agglomerate and hence the notion that porosity is mainly due to CNT agglomeration is justified. SEM micrographs are in accordance with the density results discussed later where decreasing density was observed with increasing CNT content at all sintering temperatures.

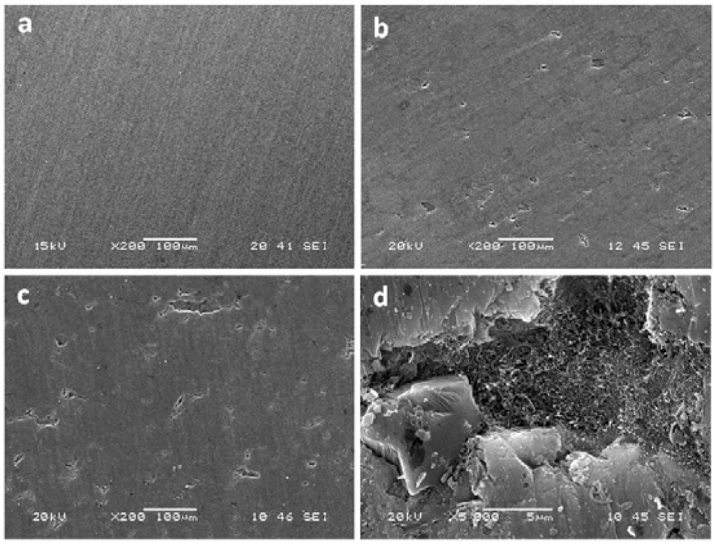

Figure 6. SEM micrographs of SPS'ed Al6061 specimens sintered at 450 °C containing (a) 0 (b) 1 and (c) 2 wt. % CNTs. (d) Magnified image of one of the pores visible in (c).

Fractured surfaces of the nanocomposite were observed and micrographs are shown in figure 7 (a and b). In figure 7 (a), 1 wt. % CNTs were found to be better dispersed into matrix and pulling out of CNTs from the fractured surface (marked with arrow) can also be seen. Whereas, figure 7 (b) shows fractured surface in case of 2 wt. % CNTs where higher degree of agglomeration is evident along with CNT pull out effect.

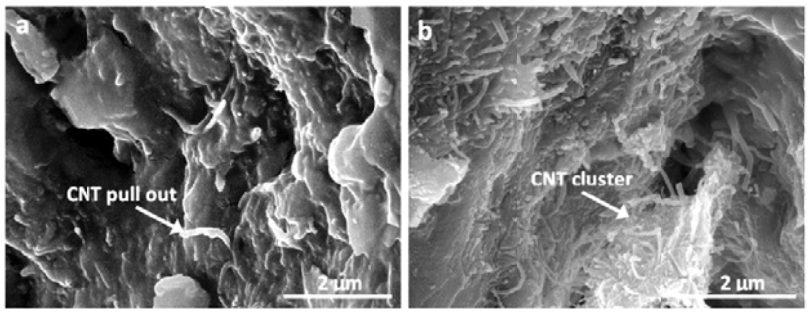

Figure 7. SEM micrographs of fractured Al6061 specimens sintered at 500 °C containing (a)1 wt. % and (b) 2 wt % CNTs

Figure 8 shows hardness and density of nanocomposites as a function of CNT content at different sintering temperatures. It can be seen that density remained considerably low at a sintering temperature of 400 °C (figure 8 a and d). However, it increased significantly as the temperature was increased to 450 °C (figure 8 b and e). An increase in the temperature to 500 °C (figure 8 c and f) promoted densification for nanocomposites, especially for Al6061 alloy. For monolithic alloys, temperature of 450 °C is enough for complete densification but for nanocomposites, 100 % densification was hardly achieved even at 500 °C. However, improvement in densification is significant as the temperature increased from 400 to 450 and 500 °C. This is owing to the fact that sintering is a thermally activated process controlled primarily by diffusion. Therefore, the higher sintering temperature the higher the diffusion rate and the higher the rate of porosity elimination. Also, it is well known that in SPS, the electric pulse (DC) discharge generates spark plasma between the particles and resulting joule heating promotes densification [13, 18-20]. The formation of plasma during SPS has direct effect on generating heat which results in neck growth between adjacent particles in the powder mixture. However, the exact phenomenon is still having critical discussion amongst researchers [13, 21]. The overall trend shows that the sintered composites displayed good densification and high relative densities and this is due to the fact that field assisted consolidation methods such as SPS are capable of providing high instantaneous energy for sintering nanocomposites compared to other conventional sintering techniques.

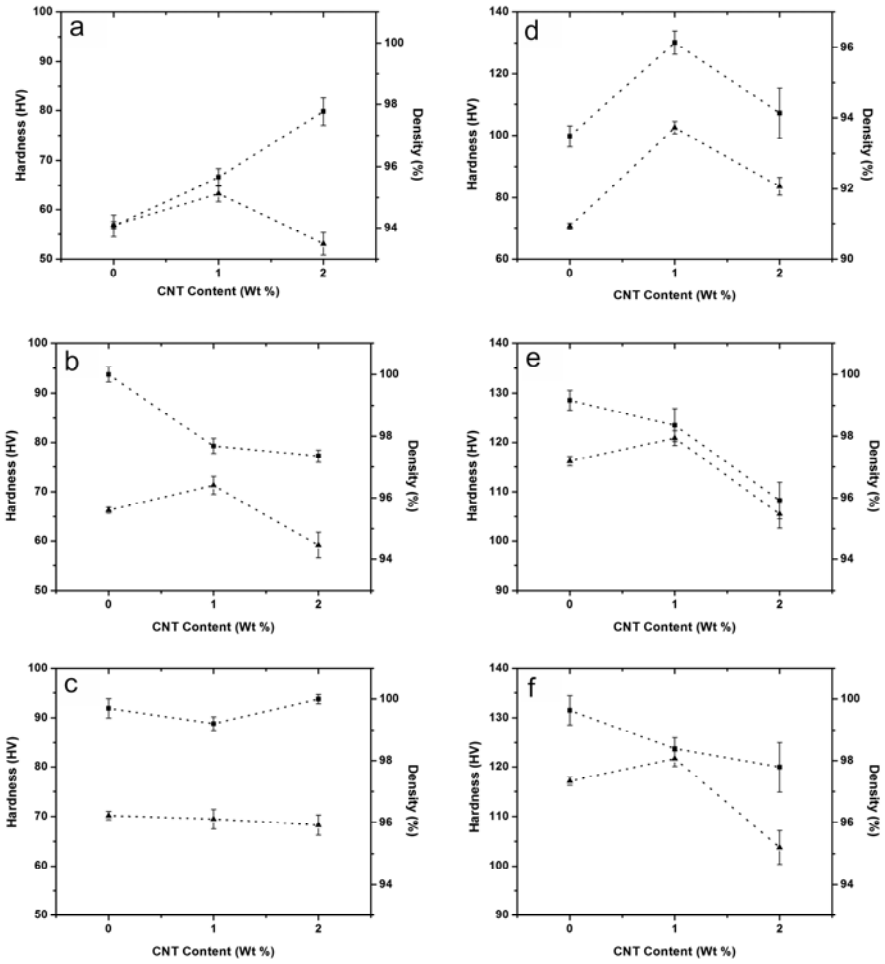

Figure 8. Hardness (▲) and density (■) of (a, b and c) Al6061 and (d, e and f) Al2124 alloys as a function of CNT content at sintering temperatures of 400 °C (a and d), 450 °C (b and e) and 500 °C (c and f).

Figure 8 also shows Vicker's microhardness of nanocomposites as a function of CNT content at different sintering temperatures. The change of microhardness with sintering temperature matched the change of relative density as a function of sintering temperature and this is due to the fact that both relative density and microhardness are dependent upon the percent porosity present in the material. Increase of CNT content up to 1 wt. % resulted in increase of the hardness of the samples. A further increase of CNT content up to 2 wt. % caused the decrease of the microhardness to values lower than the value of monolithic alloys.

The above results show that 1 wt. % CNTs is an optimum content for maximum hardness of the Al6061 and Al2124 alloys and CNT content as high as 2 wt. % results in dramatic decrease of hardness. Esawi *et. al.*, [9] reported enhancement in mechanical properties upon addition of lower proportion of CNTs, but for higher CNT contents, opposite trend was observed which was attributed to the presence of CNT clusters. Also, Kim et al. [22] found highest hardness and wear resistance for Al in case of 1 wt. % CNTs and for higher CNT content, poor properties were attributed to CNT agglomeration and formation of aluminum carbide. Also, maximum tensile and compressive properties were reported [11] for 0.5 wt. % CNTs and decreasing trend was observed for much higher CNT proportions.

4 Conclusion

Al\CNT nanocomposites were successfully prepared using probe sonication and wet ball milling followed by SPS. Less agglomeration of CNTs, good densification, and better hardness were achieved for composites containing 1 wt. % CNTs. However, composites containing 2 wt. % CNTs had excessive agglomeration of CNTs and poor hardness. Therefore, 1 wt. % CNTs is an optimum content for obtaining highly dense and hard Al6061 and Al2124 nanocomposites.

Acknowledgement

The authors would like to acknowledge financial support from King Abdul Aziz City for Science and Technology (KACST) through research project number ARP-28-122.

References

[1] Iijima S. Helical microtubules of graphitic carbon. *Nature*, **354**, pp. 56-58 (1991).
[2] Wong E.W, Sheehan P.E, Liebert C.M. Nanobeam mechanics: elasticity, strength, and toughness of nanorods and nanotubes. *Science*, **277**, pp. 1971-1975 (1997).
[3] Kuzumaki T, Miyazawa K, Ichinose H, Ito K. Processing of Carbon Nanotube Reinforced Aluminum Composite. *Journal of Materials Research*, **13**, pp. 2445-2449 (1998).
[4] Salas W, Alba-Baena N.G, Murr L.E. Explosive Shock-Wave Consolidation of Aluminum Powder/Carbon Nanotube Aggregate Mixtures: Optical and Electron Metallography. *Metallurgical and Materials Transactions A*, **38**, pp. 2928-2935 (2007).
[5] Morsi K, Esawi A.M.K, Borah P, Lanka S, Sayed A. Characterization and Spark Plasma Sintering of Mechanically Milled Aluminum- Carbon Nanotube (CNT) Composite Powders. *Journal of Composite Materials*, **44**, pp. 1991-2003 (2010).
[6] Laha T, Chen Y, Lahiri D, Agarwal A. Tensile properties of carbon nanotube reinforced aluminum nanocomposite fabricated by plasma spray forming. *Composites Part A: Applied Science and Manufacturing*, **40**, pp. 589-594 (2009).
[7] Kwon H, Hoon D, François J, Kawasaki A. Investigation of carbon nanotube reinforced aluminum matrix composite materials. *Composites Science and Technology*, **70**, pp. 546-550 (2010).
[8] Wu Y, Kim, G.Y. Carbon nanotube reinforced aluminum composite fabricated by semisolid powder processing. *Journal of Materials Processing Technology*, **211**, pp. 1341-1347 (2011).

[9] Esawi A, Elborady M. Carbon nanotube-reinforced aluminium strips. *Composites Science and Technology*, **68**, pp. 486-492 (2008)
[10] Esawi A.M.K, Morsi K, Sayed A, Taher M, Lanka S. Effect of carbon nanotube (CNT) content on the mechanical properties of CNT-reinforced aluminium composites. *Composites Science and Technology*, **70**, pp. 2237-2241 (2010).
[11] Liao J.Z, Tan M.J, Sridhar I. Spark plasma sintered multi-wall carbon nanotube reinforced aluminum matrix composites. *Materials and Design*, **31**, pp. S96- S100 (2010).
[12] Choi H.J, Lee S.M, Bae D.H. Wear characteristic of aluminum-based composites containing multi-walled carbon nanotubes. *Wear*, **270**, pp. 12-18 (2010).
[13] Orrù R, Licheri R, Locci A.M, Cincotti A, Cao G. Consolidation/synthesis of materials by electric current activated/assisted sintering. *Materials Science and Engineering R,* **63**, pp. 127-287 (2009).
[14] Munir, Z.A., Anselmi-Tamburini U, Ohyanagi M. The effect of electric field and pressure on the synthesis and consolidation of materials: A review of the spark plasma sintering method. *Journal of Materials Science*, **41**, pp. 763-777 (2006).
[15] Khalil A, Hakeem A.S, Saheb N. Optimization of Process Parameters in Spark Plasma Sintering Al6061 and Al2124 Aluminum Alloys. *Advanced Materials Research*, **328-330**, pp. 1517-1522 (2011).
[16] Saheb N. Spark Plasma Sintering of Al6061 and Al2124 Alloys. *Advanced Materials Research*, **284-286**, pp. 1656-1660 (2011).
[17] Saheb N. Effect of Processing on the Dispersion of CNTs in Al-Nanocomposites. *Advanced Materials Research,* **239-242**, pp. 759-763 (2011).
[18] Viswanathan V, Laha T, Balani K, Agarwal A, Seal S. Challenges and advances in nanocomposite processing techniques. *Materials Science and Engineering* R, **54**, pp. 121-285 (2006).
[19] Adachi J, Kurosaki K, Uno M, Yamanaka S. Porosity influence on the mechanical properties of polycrystalline zirconium nitride ceramics. *Journal of Nuclear Materials*, **358**, pp. 106-110 (2006).
[20] Jin X, Gao L, Sun J. Preparation of nanostructured $Cr_{1-x}Ti_xN$ ceramics by spark plasma sintering and their properties. Acta Materialia **54**, pp. 4035-4041 (2006).
[21] Kim Y.H, Sekino T, Kusunose T, Nakayama T, Niihara K, Kawaoka H. Electrical and Mechanical Properties of K, Ca Ionic-conductive Silicon Nitride Ceramics*. Ceramic Transactions*, **165**, pp. 31-38 (2005).
[22] Kim I.Y, Lee J.H, Lee G.S, Baik S.H, Kim Y.J, Lee Y.Z. Friction and wear characteristics of the carbon nanotube-aluminum composites with different manufacturing conditions. *Wear*, **267**, pp. 593-598 (2009).